

Supporting Information

Probing the PEDOT:PSS/Cell Interface with Conductive Colloidal Probe AFM-SECM

P. Knittel, H. Zhang, C. Kranz, G. G. Wallace and M. J. Higgins

1. Fabrication of Colloidal AFM-SECM Probes

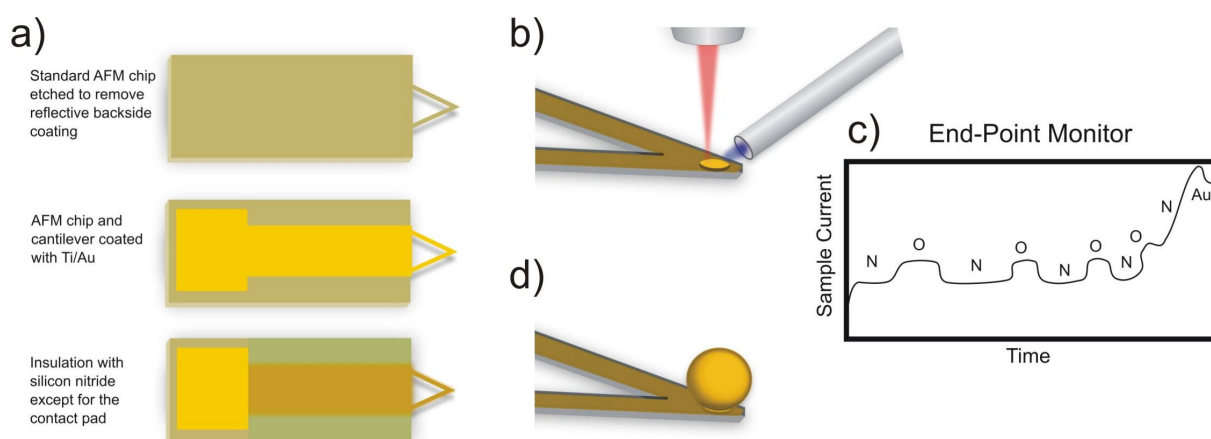


Fig. S1. Scheme of fabrication process for AFM-SECM probes. a) Commercially available silicon nitride AFM probes were etched in aqua regia and chrome etchant to remove the backside coating. A Ti/Au layer was deposited onto the cantilever and the chip using a stainless steel shadow mask. Partial (no coating on the contact pad) or complete insulation of the chip was obtained with e.g. mixed layers of silicon nitride/silicon dioxide. b) Selective removal of the insulation using gas-assisted (XeF_2) FIB milling to expose an electrode at the modified AFM tip. Etching through a mixed silicon nitride/silicon dioxide (denoted as N and O) layer can be easily followed using the End-Point Monitor c), which records the specimen current over time. Silicon nitride and dioxide layers can be clearly distinguished in the beginning. Reaching the buried gold layer, the current rises drastically (scheme shows a smaller increase for scaling reasons) until reaching a climax, where the ion beam starts milling the Au layer and hence, the patterning is stopped. Afterwards a colloid was attached to the exposed electrode as shown in d).

2. Electrochemical Characterization

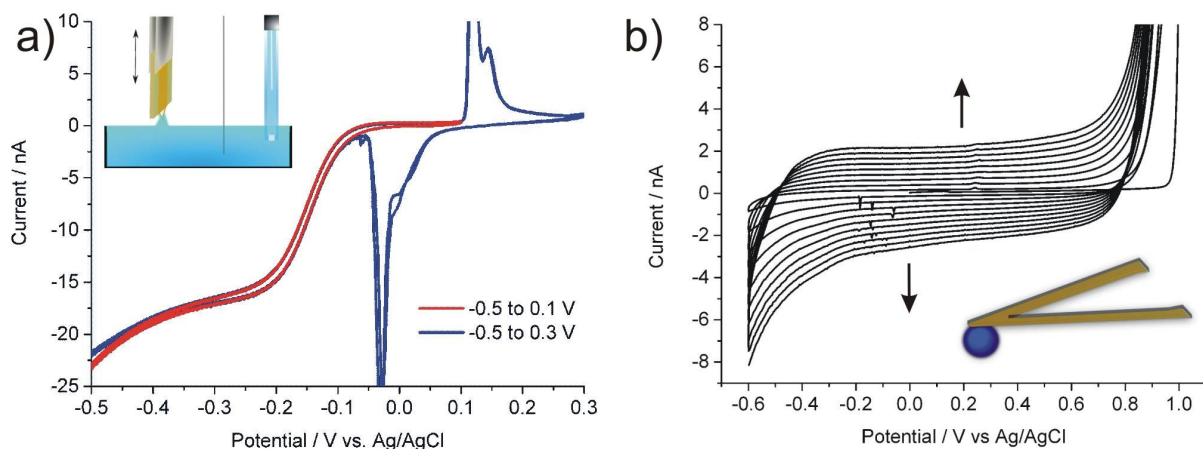


Fig. S2. a) Electrochemical characterization of the cantilevers after attaching a colloid with exposed silver in 10 mM $[\text{Ru}(\text{NH}_3)_6]\text{Cl}_3/0.1\text{M KCl}$. Due to the manufacturing process, the colloids also have an Ag layer underlying the gold so that the oxidation and reduction peaks of Ag may be visible at 0.14 V and 0 V vs. silver/silver chloride (Ag/AgCl; (sat. KCl)) at some colloids, indicating an incomplete gold coverage. However, the silver redox couple is outside of the potential scan range for the redox mediator $[\text{Ru}(\text{NH}_3)_6]\text{Cl}_3$. The red curve shows a small potential range where no silver oxidation/reduction is visible as compared to the blue curve recorded in a larger potential range. Inset shows three-electrode setup for electrochemical measurements displaying the cantilever as working electrode and the reference and counter electrode. The cantilever connected with a stainless steel clamp is carefully immersed into the solution using a z-positioner; b) shows the current response of the PEDOT:PSS deposition in 10 mM EDOT/ 0.1 mM NaPSS (scan rate 100 mV/s) with rising currents for each subsequent cycle.

3. Raman Spectrum of PEDOT:PSS on the Colloid

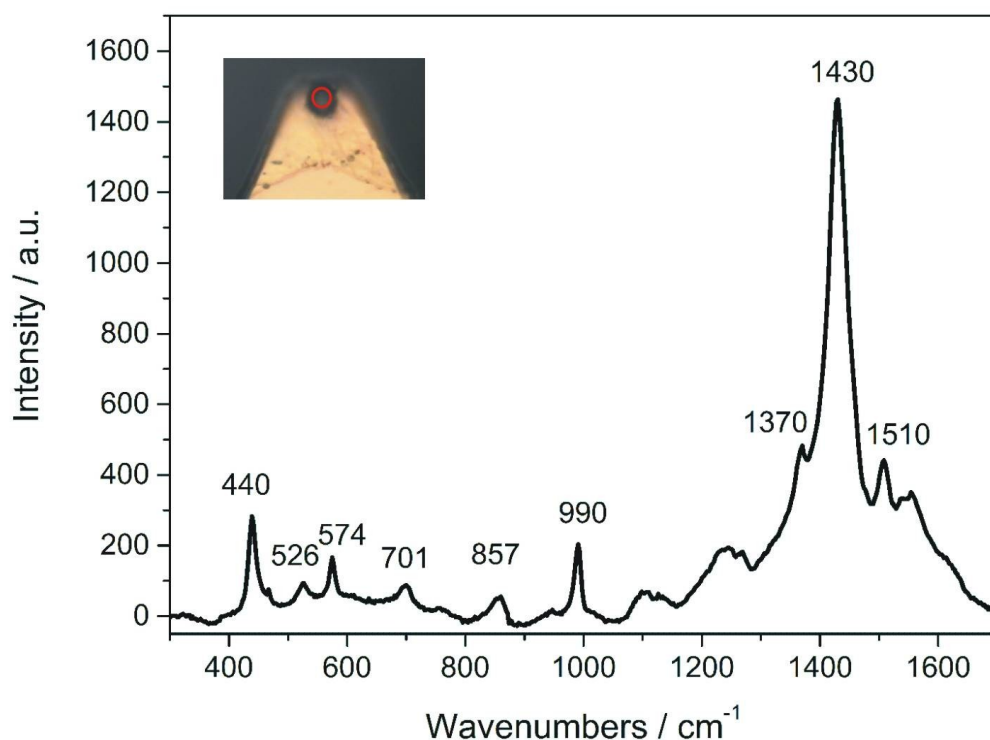


Fig. S3. The Raman spectra of the deposited polymer revealed bands of PEDOT:PSS at 1510, 1430, 1370, 990, 857, 701, 574, 526, 440 cm^{-1} respectively, which can be assigned to C=C stretching (asymmetric at 1510 cm^{-1} , symmetric C=C(-O) at 1430 cm^{-1}), $\text{C}_\beta\text{-C}_\beta$ stretching (1370 cm^{-1}), oxyethylene ring deformation (990, 574, 440 cm^{-1}), asymmetric C-S-C deformation (701 cm^{-1}), as reported in literature¹. The inset shows the microscope image of the cantilever with the modified colloid and the measurement region (red circle).

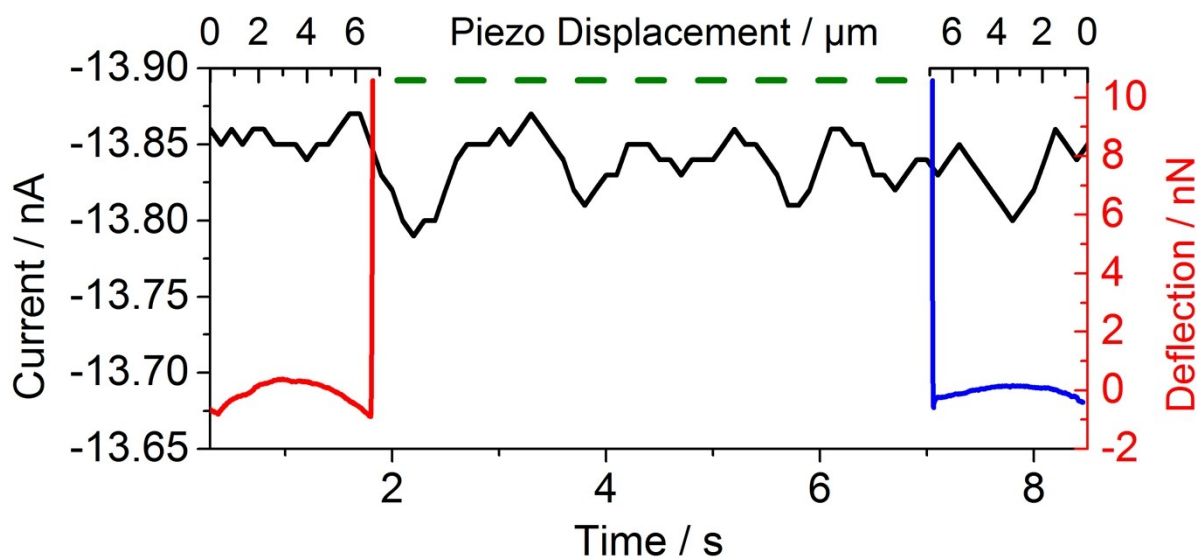


Fig. S4. Simultaneously recorded Faradaic current (tip potential – 0.6 V vs. Ag/AgCl, and cantilever deflection and piezo displacement of a single force curve (setpoint 10 nN) on the PPy substrate surrounding the fibroblast cells during measurement. In contrast to the measurements on the cells no current drop was recorded..

7. References

- 1 S. Sakamoto, M. Okumura, Z. Zhao and Y. Furukawa, *Chem. Phys. Lett.*, 2005, **412**, 395–398.